Eur. Phys. J. A **17**, 285–296 (2003)
DOI 10.1140/epja/i2002-10152-3

THE EUROPEAN PHYSICAL JOURNAL A

Precise measurement of the ^{27}Al(n, 2n)^{26g}Al excitation function near threshold and its relevance for fusion-plasma technology

A. Wallner[1,a], S.V. Chuvaev[2], A.A. Filatenkov[2], Y. Ikeda[3], W. Kutschera[1], G. Mertens[4], A. Priller[1], W. Rochow[4], P. Steier[1], and H. Vonach[1]

[1] Institut für Isotopenforschung und Kernphysik, University of Vienna, Währinger Str. 17, A-1090 Wien, Austria
[2] V.G. Khlopin Radium Institute, 2nd Murinski ave. 28, 194021 St. Petersburg, Russia
[3] Fusion Neutronics Laboratory (FNS), Department of Reactor Engineering, Japan Atomic Energy Research Institute, Tokai-mura, Ibaraki-ken 319-1195, Japan
[4] Physikalisches Institut, University of Tübingen, Auf der Morgenstelle 14, D-72076 Tübingen, Germany

Received: 26 November 2002 / Revised version: 28 February 2003 /
Published online: 27 May 2003 –
Communicated by M. Garçon

Abstract. A new accurate measurement of the ^{27}Al(n,2n)^{26}Al excitation function leading to the ground state of ^{26}Al ($t_{1/2} = 7.1 \times 10^5$ years) in the near-threshold region ($E_{\rm th} = 13.55$ MeV) was performed, with the goal to achieve relative cross-sections with the highest accuracy possible using proven methods. In addition, the measurements were also designed to provide good absolute cross-section values, since absolute cross-sections are important for radioactive waste predictions in future fusion reactor materials. Samples of Al metal were irradiated with neutrons in the energy range near threshold ($E_{\rm n} = 13.5$–14.8 MeV) in Vienna and St. Petersburg, and at 14.8 MeV in Tokai-mura. In addition, irradiations with neutrons of higher energies (17 and 19 MeV) were performed in Tübingen, to obtain also cross-section values well above threshold. The amount of ^{26}Al produced during the irradiations was measured via accelerator mass spectrometry (AMS). With this system, a background as low as 3×10^{-15} for ^{26}Al/^{27}Al isotope ratios was obtained, corresponding to a (n,2n) cross-section of 0.04 mb. Utilizing AMS, cross-sections with much higher precision and considerably closer to the threshold than in previous investigations were measured. A substantial improvement in the knowledge of this excitation function was obtained. Its expected strongly non-linear behaviour near threshold makes the production of ^{26}Al sensitive to temperature changes in a deuterium-tritium (D-T) fusion plasma. The prerequisite for such an application as a temperature monitor, namely a very well-known shape of the excitation function, was met. A quantitative prediction of the sensitivity of this method for monitoring the temperature in a D-T fusion plasma was therefore possible.

PACS. 07.75.+h Mass spectrometers – 28.20.+v Neutron physics – 28.52.-s Fusion reactors – 52.70.Nc Plasma diagnostic techniques and instrumentation: Particle measurements

1 Introduction

The production of the long-lived radionuclide ^{26}Al is of considerable interest for fusion technology [1–3]. In a deuterium-tritium (D-T) fusion plasma 14 MeV neutrons are generated. The closeness of this energy to the threshold of the ^{27}Al(n,2n)^{26g}Al reaction ($E_{\rm th} = 13.55$ MeV) manifests itself in two different ways. On the one hand, the neutron bombardment of aluminum and silicon bearing materials lead to a built-up of ^{26}Al activity. On the other hand, the sensitivity of the ^{26}Al activity on the temperature-dependent neutron energy distribution leads to the possibility of utilizing the ^{27}Al(n,2n)^{26}Al reaction for a plasma temperature measurement. It is this second aspect, which has initiated us to remeasure the excitation function with much higher precision than previously known. First results of these measurements have already been reported in [4]. An extended description of the whole study of the ^{27}Al(n,2n)^{26}Al excitation function may be found in ref. [5].

1.1 The production of ^{26}Al via neutron activation

The long half-life of the ground state of ^{26}Al ($t_{1/2} = (7.1 \pm 0.2) \times 10^5$ y, [6]) makes this nuclide an activation

[a] *Present address*: Accelerator Laboratory of the LMU and TU Munich, Institute for Radiation Biology, LMU Munich, Am Coulombwall 6, D-85748 Garching, Germany; e-mail: anton.wallner@physik.tu-muenchen.de

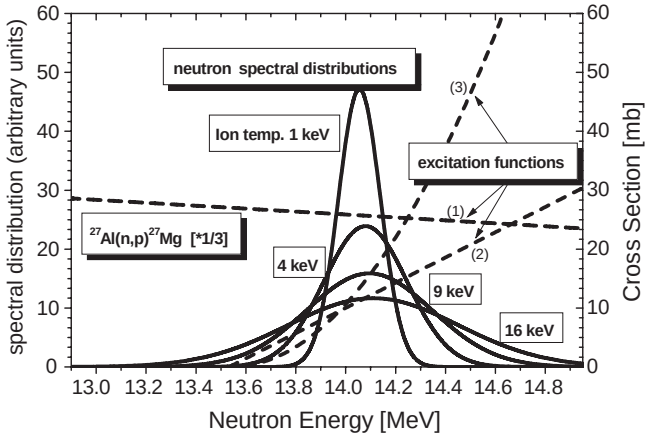

Fig. 1. Neutron spectral distribution from the T(d,n)^{4}He reaction calculated for 4 different ion temperatures (solid lines) as taken from [1] and [8]. The curves are normalized to the same area. Also shown are the presumed linear (2) and non-linear (3) shape of the excitation function for the ^{27}Al(n,2n)^{26g}Al reaction and the almost energy-independent excitation function (1) of the ^{27}Al(n,p)^{27}Mg reaction (dashed lines, cross-sections are shown on the right axis).

product, which accumulates steadily during the lifetime of a fusion reactor [1]. The neutron-induced reactions, ^{27}Al(n,2n)^{26}Al and ^{28}Si(n,np+d)^{27}Al(n,2n)^{26}Al are the main processes for the formation of ^{26}Al in deuterium-tritium (D-T) fusion environment. In order to estimate the production of ^{26}Al in such an environment, an accurate excitation function for the ^{27}Al(n,2n)^{26g}Al reaction is necessary, particularly for the strongly non-linear behavior expected for (n,2n) reactions. This then allows one to make accurate predictions of the built-up of ^{26}Al and its significance for long-term waste disposal [2,3].

1.2 Applicability of the ^{27}Al(n, 2n)^{26g}Al reaction for ion-temperature measurements

An application of this reaction has been pointed out by Smither *et al.* [1,7,8]: The production rate of the long-lived ground state of ^{26}Al through the ^{27}Al(n,2n)^{26}Al reaction can in principle be used to monitor the ion temperature in a D-T fusion plasma. Existing measurements of ^{27}Al(n,2n)^{26g}Al cross-sections, however, are strongly discordant (see sect. 1.3) and by far insufficient to determine the shape of the excitation function with the needed accuracy. As a result, they do not allow one to make predictions about its usefulness for the above-mentioned purpose.

In a D-T fusion plasma the deuterium-tritium reaction produces alpha-particles and neutrons. The neutron energy distribution itself is a sensitive function of the plasma ion temperature. In a purely thermal plasma the width and centroid of this neutron spectral distribution are directly connected to the ion temperature of a D-T (and also D-D) fusion plasma: The energy spectrum of neutrons produced in nuclear fusion reactions has a Gaussian form with a centroid at 14.1 MeV. The width of the energy distribution is proportional to the square root of the ion temperature (fig. 1). If the ion temperature changes, then the neutron spectral distribution shows a small shift of the centroid but a considerable change of the width.

The yield of a reaction induced with neutrons of a finite energy distribution for different ion temperatures depends strongly on the shape of the excitation function in the energy region of interest.

$$P = N \int_{E_0}^{E_{\max}} \sigma(E_\mathrm{n})\phi(E_\mathrm{n})\mathrm{d}(E_\mathrm{n})\,. \qquad (1)$$

The production rate P can be determined as the integral over the neutron energy range $[E_0, E_{\max}]$ of the product of the target particles N times the cross-section $\sigma(E_\mathrm{n})$ and the neutron flux distribution $\phi(E_\mathrm{n})$. Smither *et al.* [1, 7,8] discussed already the production for different cases:

Investigating the production rate P of a reaction in such an environment one can distinguish 3 different cases of excitation functions (see fig. 1):

1) a linear excitation function, without threshold in this energy region
2) a second linear excitation function, but starting with a threshold within the energy region of the neutrons emitted in a D-T plasma,
3) and a quadratic (or strong non-linear) shape, again with its threshold in this energy region.

The integral yield of a reaction (total production) is proportional to the integral of the product of the neutron flux distribution and the excitation function. In the first case —the linear excitation function— the total yield *per neutron* will change very little with increasing temperatures. More neutrons at the lower and at the higher energy side will on average give the same production rate. This is true for a symmetric shape of the spectral distribution and if the centroid remains constant.

For the second case, with its threshold within the energy region, where the excitation function is rising suddenly above this energy, in principle the same temperature dependence occurs. Only, if there is an excess of neutrons with energies below the threshold a change of the yield becomes significant.

In the last case, a non-linear shape of the excitation function is assumed: If the threshold of a reaction is at or very near the centroid of the neutron energy distribution, then the yield of the reaction is quite insensitive to the lower-energy half of the distribution. The spreading of the neutron energy distribution into higher energies with increasing ion temperatures will contribute much more to the production and this effect will not be cancelled by the lower production rate due to the low-energy neutrons [1].

This strong asymmetry in the sensitivity of the low- and high-energy parts of the energy distribution makes a non-linear reaction useful for temperature determinations. The temperature sensitivity is most pronounced if —beside non-linearity— also the threshold falls within the energy region of the emitted neutrons. These features are in principle given by the ^{27}Al(n,2n)^{26}Al reaction leading to the ground state of ^{26}Al: The threshold of the Al(n,2n)

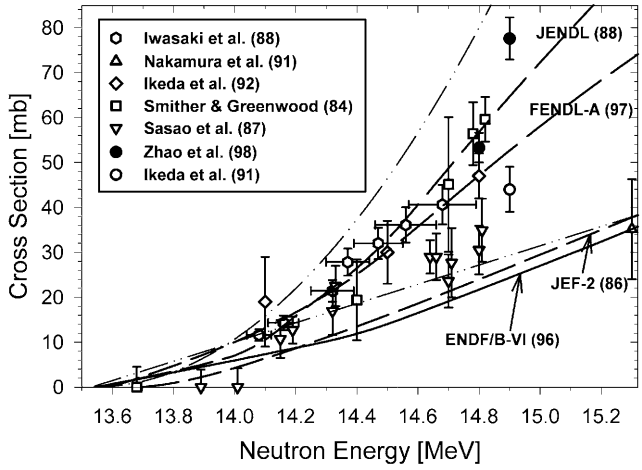

Fig. 2. Previous results for the excitation function of the ^{27}Al(n,2n)^{26g}Al reaction near threshold. The symbols indicate experimental cross-section data, the long-dashed lines and the solid one represent semi-empirical evaluations, and the dash-dotted lines show upper and lower limits for the excitation function (cf. excitation function curves in fig. 1).

reaction lies at $E_n = 13.55$ MeV. The applicability of the ^{27}Al(n,2n)^{26}Al reaction for its use to determine the temperature in a D-T plasma requests this non-linearity over the major region of neutron energies (13 to 15 MeV).

1.3 Previous measurements

Previous experiments for the determination of the ^{27}Al(n,2n)^{26g}Al cross-sections with the production of the long-lived ^{26}Al ground state (5^+) were reported between the years 1983 and 1998 utilizing both activation and AMS measuring techniques [1,7–13]. The experimental data prior to this work are shown in fig. 2. Also plotted are some semi-empirical evaluation curves [14]. No clear trend for the shape of the excitation function can be deduced from these data. The scatter in experimental data is reflected in the evaluated data files which differ by factors up to three. Upper and lower limits for the excitation function from those data are indicated by cases 2 and 3 in fig. 1. Clearly, from existing data on cross-sections it was not possible to produce an unambiguous excitation function. And consequently, no reliable estimation of the suitability of this reaction for monitoring the ion temperature in D-T fusion plasmas could be obtained.

Therefore, we started a project to determine this excitation function more accurately. The main purpose of this work was the systematic and precise measurement in the energy region near threshold.

2 Experimental procedure

In order to minimize systematic errors from irradiation geometry and fluence determination, which may be reflected in the previous data, neutron irradiations were performed at four laboratories under different conditions. Three different irradiations of Al samples were performed with 14 MeV neutrons: In Vienna and St. Petersburg a neutron energy range starting below threshold (E_{th} = 13.547 MeV) up to 14.84 MeV was available. In Tokai-mura the irradiation was performed at a neutron energy of 14.8 MeV. Well above threshold, a fourth neutron irradiation was performed in Tübingen with neutron energies of 17 and 19 MeV.

^{26}Al has a ground state of $J^\pi = 5^+$ and an isomeric state at 228 keV with $J^\pi = 0^+$. Since the latter decays directly via β^+ decay ($t_{1/2} = 6.3$ s) to ^{26}Mg, it had no influence on the present investigation. The number of ^{26}Al nuclei produced (N_{26}) is simply given (for mono-energetic neutrons) by

$$N_{26} = \sigma_{n,2n}(E_n) \cdot N_{27} \cdot \Phi\,, \qquad (2)$$

where N_{27} denotes the number of ^{27}Al atoms. The activity of ^{26}Al is very low for available neutron fluences Φ. Only in one case the activity of ^{26}Al samples was measured directly (Tokai-mura samples). In all other cases the isotope ratio N_{26}/N_{27} was determined via accelerator mass spectrometry (AMS, sect. 2.2). With this method a very sensitive tool was employed allowing a cross-section determination much more accurate compared to the activity method.

The determination of the ^{27}Al(n,2n)^{26g}Al excitation function consists of the following steps:

- During the neutron irradiations the neutron fluence Φ was obtained for all Al samples from a monitor reaction. The ^{93}Nb(n,2n)^{92m}Nb reaction was used to monitor the neutron fluence for irradiations with 14 MeV neutrons. In the case of 17 MeV and 19 MeV neutrons, Ni samples were used for the fluence determination (sect. 2.1).
- The neutron energy was determined from the irradiation geometry and checked with proven methods (sect. 2.1.1).
- With AMS the isotopic ratio N_{26}/N_{27} was determined. The measurement of the isotope ratio is independent of the sample mass. Typical sample masses of only a few mg were required, and consequently a high sample throughput was possible with this method.

2.1 Neutron irradiation and fluence determination

In the case of 14 MeV neutrons the fluence was obtained from Nb samples placed nearby the Al samples and irradiated simultaneously. Utilizing the production of ^{92m}Nb via the ^{93}Nb(n,2n)^{92m}Nb reaction for the fluence determination is straightforward because of its convenient half-life (10.15 d), the well-known cross-sections, its independence from the neutron energy around 14 MeV, and the simple decay characteristics as well as no interference from other competing reactions. Its cross-section values are nearly constant for the whole energy range of interest [15]. The total uncertainty in the fluence determination was less than 3%.

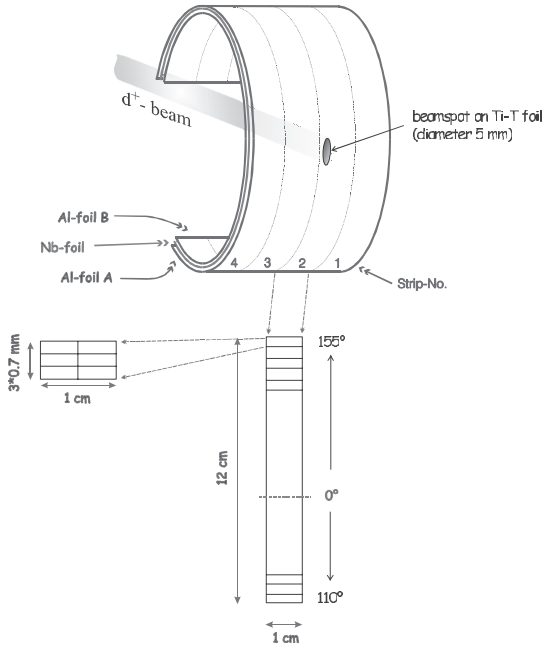

Fig. 3. Sketch of the cylindrical arrangement used for the two Al foils and the Nb foil for the irradiation in Vienna. The latter was used for the neutron fluence determination. All three foils were cut after the irradiation. The Al foils were cut into samples fitting the sample holder for the AMS measurement. The four strips with 12 cm length were divided into small samples of 0.5 mm length (or 0.25 mm) and about 0.7 mm width (see left side of the lower part). The Al foils had a thickness of 1 mm, the Nb foil of 0.125 mm.

2.1.1 Irradiation in Vienna

In the neutron energy range from 13.4 to 14.8 MeV, irradiations were performed at the Cockcroft-Walton type neutron generator of the Radium Institute in Vienna. The neutrons were produced via the fusion reaction T(d,n)^{4}He with deuterons of an energy of 230 keV. A special low-mass construction was manufactured in order to reduce the amount of scattered neutrons. In combination with the high threshold of the ^{27}Al(n,2n)^{26}Al reaction scattering from the target construction and the surrounding was assumed to be negligible.

Pure Al metal samples[1] (99.999%) with a thickness of 1 mm were used for the irradiation. Two continuous foils were placed cylindrically around the neutron producing Ti-T target at a distance of 25.5 and 26.8 mm, respectively. A Nb foil identically dimensioned was sandwiched by these Al foils (see fig. 3). The foil dimension was 4 cm in width (horizontal) and about 12 cm in length; the latter is responsible for the circumference of the partial cylinder. These foils superimposed a range of emission angles from $-110\,^\circ$ relative to the incoming d$^+$-beam and up to $+155\,^\circ$. The whole energy range available started below the threshold of the (n,2n) reaction, spanned a total of about 1.4 MeV and was available twice between 14.0 MeV and 14.82 MeV. The total irradiation time was three weeks.

The Al samples irradiated in Vienna allowed the determination of individual cross-section data. In combination with the very small sample size needed for the AMS measurements (see fig. 3), a very fine "energy resolution" was possible. After the irradiation the Nb foil was cut into small pieces. The activity of those Nb samples was determined with a HP-Ge γ-ray detector. A total neutron fluence in the order of 10^{14} n cm^{-2} was achieved (see table 1).

It is essential to know the neutron energy accurately in a measurement of a reaction cross-section that varies sharply with energy. Since this neutron energy was determined by the irradiation geometry, the corresponding irradiation angles of all samples had to be determined. A Monte Carlo code [16] was then used to calculate both the mean neutron energy and the neutron spectral distribution for this specific irradiation arrangement. To this end, an energy loss of 10 ± 10 keV in a T-depleted zone was assumed for the deuterons entering the target. The T concentration was taken to be constant with a T : Ti ratio of 1.5 ± 0.5.

The neutron energy was also checked via the Zr-Nb method [17]: A combination of the ^{93}Nb(n,2n)^{92m}Nb cross-section with that of the ^{90}Zr(n,2n)$^{89m+g}$Zr reaction can be used for an energy standard. Their well-known cross-section ratio varies strongly over the energy region of interest. The neutron energy scale was so verified by measuring the ratio of the ^{89}Zr to ^{92m}Nb specific activities induced in Zr and Nb foils, which were exposed to neutrons as a sandwich Zr-Nb-Zr at the backside of the Al foils at ten different positions over the entire length of the Al foils (not shown in fig. 3). Overall 40 Zr-Nb-Zr sandwiches were irradiated, each a few days. Therefore, a check for possible deviations in the sample-target arrangement was given for the whole irradiation. In addition, stacks of yttrium foils and Nb foils were used for an efficiency check of the HP-Ge γ-ray detector by the comparison of the γ-ray detector with a well-type NaI(Tl) detector. This was important to determine absolute values for the neutron fluence.

A very good agreement was found between the two neutron energy determinations. It was confirmed that the discrepancy was not larger than 20 keV for the whole 14 MeV energy region.

2.1.2 Irradiation in St. Petersburg

Al samples were irradiated using the neutron generator NG-400 of the Khlopin Radium Institute (KRI) in St. Petersburg [18,19]. ^{27}Al(n,2n)^{26g}Al reaction cross-sections could be determined for eight neutron energy values in the interval from 13.5 to 14.9 MeV for rigidly fixed standard conditions (see, *e.g.*, ref. [19]). The distance from the target to the front of the sample package was 25 mm and the deuteron energy was 300 keV. In contrast to the irradiation in Vienna, individual Al samples were irradiated. The size of an individual sample was 14 mm in diameter and 1 mm thickness. Nb samples were used for the fluence

[1] Goodfellow Cambridge Limited.

Table 1. Summary of the experimental conditions for the four neutron irradiations of Al metal samples using the T(d,n)^{4}He reaction. For all samples, the ^{26}Al content was measured via AMS at VERA.

	Vienna	St. Petersburg	Tokai-mura	Tübingen
d^+ energy (keV)	230	300	400	1200 and 2600
Irradiation angle	(−100°)–0°–(+160°)	0°–150°	20°	0°
Neutron energy range (MeV)	13.95–14.82–13.45	14.83–13.47	14.80	17 + 19
Irradiation geometry	cylindrical (4*12 cm^2)	8 positions	1 position	1 position
Sample arrangement	Al-Nb-Al	Nb-Al-Nb-Al-Nb	5*Al-Nb	Ni-Al-Ni-Al-Ni
Distance from target (mm)	26	25	7	14
Fluence determination	^{93}Nb(n,2n)^{92m}Nb	^{93}Nb(n,2n)^{92m}Nb	^{93}Nb(n,2n)^{92m}Nb	^{58}Ni → ^{57}Co$_{prod}$
Typical neutron fluence (n cm^{-2})	1.4×10^{14}	1.5×10^{14}	5×10^{16}	1.2×10^{12}
Irradiation time (d) of Al samples	20	20	5	4 and 8
AMS samples measured	157	102	84	40
Expected ^{26}Al/^{27}Al isotope ratio	$\leqslant 6 \times 10^{-12}$	$\leqslant 6 \times 10^{-12}$	$\approx 1.5 \times 10^{-9}$	$\approx 1 \times 10^{-13}$

determination, too. Stacks of samples in the order Nb-Al-Nb-Al-Nb were used. The total neutron fluence obtained was again about 1.5×10^{14} n cm^{-2}. Two Al samples per neutron energy point were available. The neutron energy was well defined utilizing cross-checks from former irradiations and applying the same fixed irradiation conditions. In addition, similarly to the irradiation in Vienna, a few Zr-Nb sandwiches have been irradiated for a check of the neutron energy (see sect. 2.1.1).

2.1.3 Irradiation in Tokai-mura

Another neutron irradiation of Al samples was performed at the Fusion Neutronics Source (FNS) [20] of the Japan Atomic Energy Research Institute in Tokai-mura. Al foils were irradiated with neutrons with a mean neutron energy of (14.80 ± 0.05) MeV. The high neutron fluence (10^{16} n cm^{-2}) made it possible to determine the ^{26}Al activity of these samples from a decay measurement, and to compare it with an independent ^{26}Al determination through AMS [21]. The neutron energy was determined by utilizing the same irradiation geometry as it has been used in former irradiations.

2.1.4 Irradiation in Tübingen

17 and 19 MeV neutrons were produced in Tübingen using a single-ended 3 MV van de Graaff accelerator. This energy region is of interest for activation calculations in fusion technology. *E.g.*, supra-thermal neutrons are produced in reactions of high-energy tritons with deuterium, where the tritons are secondary products of D-D reactions in the D-T plasma.

Deuterons with an energy of 1.2 MeV and 2.6 MeV, respectively, were produced. The distance from the d-t target was 14 mm. Al samples (1 cm in diameter, 1 mm thickness) at 0° relative to the incoming d^+-beam were irradiated. The sample arrangement consisted of a stack of foils in the succession of Ni-Al-Ni-Al-Ni (Ni foils each 0.125 mm thick). The finite width of the neutron energy distributions (from the energy loss of the deuterium in the Ti-T target, and from geometry) was taken into account.

An irradiation time between 4 days (17 MeV) and 8 days (19 MeV) was necessary to produce a neutron fluence of about 10^{12} n cm^{-2}. For the determination of the neutron fluence, the ^{58}Ni(n,np+pn+d)^{57}Co reaction was chosen because the shape of that excitation function is similar to that of the ^{27}Al(n,2n)^{26g}Al reaction. The finite neutron spectral distribution for the neutrons of 17 and 19 MeV will have the same effect in the production rate for a similar shaped excitation function. The uncertainty of this cross-section has been recently reduced in an evaluation to 4% [22]. ^{57}Co is also produced via the ^{58}Ni(n,2n)^{57}Ni reaction with subsequent decay of ^{57}Ni to ^{57}Co. Its activity build-up from the decay of ^{57}Ni was taken into account.

2.2 AMS measurements at VERA

The amount of ^{26}Al nuclei formed in all irradiations (Vienna, St. Petersburg, Tokai-mura and Tübingen), was determined via accelerator mass spectrometry (AMS) with the Vienna Environmental Research Accelerator (VERA) [23,24]. A more detailed description of Al measurements with VERA can be found in [5,21,25].

AMS does not depend on the radioactive decay and on the total sample mass. In combination with the use of negative ions and the suppression of molecules by applying acceleration and charge exchange, AMS offers an excellent sensitivity. AMS counts the radionuclides of interest directly, and doesn't have to wait for their infrequent decays. Due to the long half-life of ^{26}Al this method offers the possibility of a very much higher throughput of Al samples as compared to an activity measurement. In addition, magnesium does not form stable negative ions at all, which allows one to suppress very effectively the otherwise overwhelming interference from the stable isobar ^{26}Mg.

After the neutron irradiation, the Al foils were cut into small pieces of $\approx 3 \times 1 \times 1$ mm^3 (a few mg mass, see fig. 3) and pressed into sample holders. Negative Al ions extracted from the Cs-beam sputter source (MC SNICS

with a 40-sample target wheel [26]) pass several mass and energy filters, are injected into the tandem accelerator, which is operated at a terminal voltage of typically 2.7 MV. At the terminal the ions pass through a stripper canal filled with a few μbar of Ar gas, which leads to positively charged ions and to the dissociation of molecules. A high-energy analyzing magnet selects the most probable charge state (3^+) of the nuclide of interest. In a short time sequence both the stable ^{27}Al and the radionuclide ^{26}Al are injected into the tandem. Insertable Faraday cups measure the ion currents of the stable $^{27}Al^{3+}$ ions, whereas the rare $^{26}Al^{3+}$ nuclei are counted with a particle detector. Typical $^{27}Al^-$ currents were in the order of a few 100 nA and the transmission of negative ions to positively charged (3^+) ions at the detector position reached 45%. An isotope ratio of a few times 10^{-12} corresponded to a count rate of ≈ 1 $^{26}Al^{3+}$ ion per second registered with the Si detector. This was the maximum count rate for Al samples irradiated in Vienna and St. Petersburg.

The ^{27}Al(n,2n)^{26g}Al cross-sections were determined in the near-threshold region, which meant that the corresponding ^{26}Al concentrations were steadily decreasing for neutron energies approaching the threshold energy, eventually dipping into the background level. For the determination of the applicability of the reaction in fusion technology an accurate knowledge particularly in the near-threshold region is essential. The background level was carefully investigated with both non-irradiated Al metal and Al oxide samples. The ^{26}Al/^{27}Al background was at a level of a few times 10^{-15} [21], which corresponds to cross-sections of about 0.04 mb. This was approximately a factor 100 lower than achieved in previous cross-section measurements (see fig. 2).

The unknown isotope ratios, measured as the dead-time corrected ratios of the $^{26}Al^{3+}$ count rates divided by the corresponding $^{27}Al^{3+}$ particle currents, have to be normalized and checked with Al standards of well-known ratios. Several different ^{26}Al standard materials covering an isotopic ratio between 5×10^{-10} and 1×10^{-12} were available. The comparison of these standard materials with each other, however, led to inconsistent results [21]. It was intended to get not only the shape of the excitation function, but also absolute cross-section data for the whole energy range needed in fusion technology for the purpose of activation calculation (see sect. 1.1). Due to the inconsistent result of the comparison of the various ^{26}Al standards, an uncertainty of more than 10% would have resulted for the absolute cross-section data. As a possible way-out an independent Al standard was produced. Al metal samples were irradiated with an exceptional high neutron fluence (Tokai-mura). This allowed the measurement of their ^{26}Al activity directly with a Ge γ-ray detector, which was compared with the values obtained from the subsequent AMS measurement [21]. This independent standard confirmed the values of the so-called Purdue standards [27], which therefore were used for the determination of the absolute scaling factor in the AMS measurement. With this independent Al metal standard the systematic error of the AMS measurement could be reduced significantly.

Al metal samples were used for the measurement of unknown isotopic ratios, whereas the Al standards were available as Al oxide powder only. We therefore converted some irradiated Al metal samples into Al oxide in order to check for possible differences in the ratio measurements. No difference in the isotope ratio was obtained compared to the result of the corresponding metal sample [21].

Several measurement series were performed for the determination of the excitation function. The ratios of all blank samples fell into the range between 1×10^{-15} and 3×10^{-15}. The ratios of the Al standards were reproduced to better than 1%. Overall, 383 irradiated Al samples were measured at VERA (see table 1).

3 Results

3.1 Cross-section data

The energy-dependent cross-sections were determined from the measured ^{26}Al/^{27}Al isotope ratio and the corresponding neutron fluence using eq. (2):

$$\sigma_{\mathrm{n,2n}}(E_{\mathrm{n}}) = \frac{^{26}\mathrm{Al}}{^{27}\mathrm{Al}} \cdot \frac{1}{\Phi}\,. \tag{3}$$

Due to the steeply increasing shape of the excitation function, the neutron energy of the cross-section data had to be corrected for the finite width of the neutron energy distribution. These neutron distributions were calculated with a Monte Carlo code [16]. Necessary for the determination of this correction was a first guess of the shape of the excitation function. This was obtained using a fit where the cross-section data were associated with the centroid of the neutron energy distribution. A rather large shift had to be applied to the "original" neutron energy in the region close to threshold which leads also to a larger uncertainty of the neutron energy in this energy region. This effect is due to the vanishing cross-sections in this region: Only that part of the spectral distribution accounts for the corrected neutron energy, which lies above threshold.

In fig. 4a all cross-section data obtained from AMS measurements on samples irradiated in Vienna are plotted. Several run series were performed (157 individual data). A blow-up of the threshold region is shown in the insert. The background level of the AMS measurements was determined from "blank" samples. Adding the one standard deviation to the blank value gave a cross-section limit of 0.04 mb. The error bars shown in the figure include the total error from the fluence determination and from the AMS measurement (random and systematic errors). Not included is the uncertainty of the neutron energy (see below). A very consistent set of individual data was obtained down to background level. The scattering of the individual results shows the precision of the measurement, which was in the order of a few percent. The individual data were averaged with a bin structure of about 0.1 MeV neutron energy. The squares in fig. 4a represent this averaged cross-section data obtained from the Vienna samples.

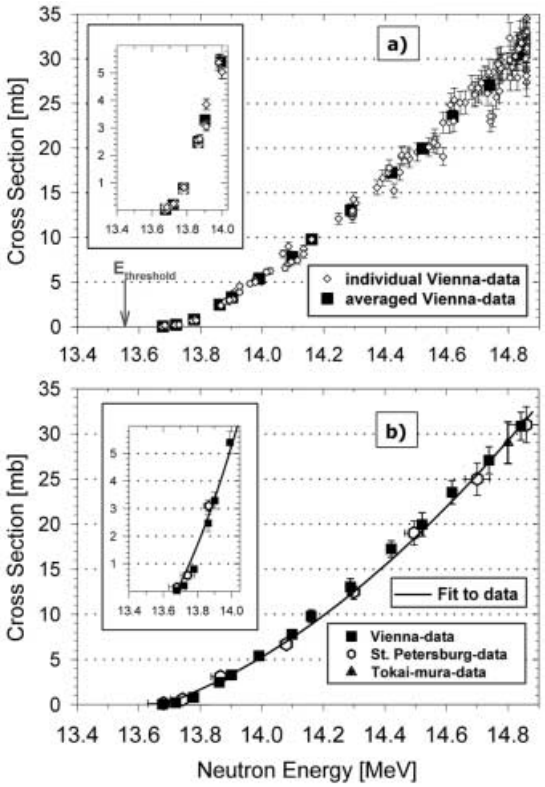

Fig. 4. Cross-section data for the ^{27}Al(n,2n)^{26g}Al excitation function in the near-threshold region. In part a) the individual data for Al samples irradiated in Vienna are plotted (small symbols) together with averaged data using a 100 keV bin structure (filled squares). In part b) these averaged Vienna data are compared with that obtained from samples irradiated in St. Petersburg (open hexagons) and that from Tokai-mura (triangle). The solid line depicts a third-order fit to the Vienna data without any constraints: $\sigma_{n,2n}(E_n) = 17081.8 - 3520.94 \times E_n + 240.0155 \times E_n^2 - 5.40300 \times E_n^3$; these results correspond to a parameterization of $\sigma_{n,2n}(E_n) = 10.8 \times (E_n - 13.67) + 20.8 \times (E_n - 13.67)^2 - 6.5 \times (E_n - 13.67)^3$.

Cross-section data from samples irradiated in St. Petersburg are plotted in fig. 4b, together with the averaged Vienna data of fig. 4a. The mean neutron energy was again corrected for the finite width of the neutron spectral distribution. For those samples irradiated in St. Petersburg, ^{26}Al/^{27}Al isotope ratios were obtained by averaging the ratio measured for the individual Al samples. These samples were part of a larger Al foil irradiated with the known neutron fluence. Figure 4b demonstrates a very good agreement between the data sets "St. Petersburg" and "Vienna". This is true down to the lowest cross-section data in the near-threshold region. The difference between both data sets is nowhere larger than 0.8 mb and all data are compatible within their errors. The error shown in this figure consists of both random and systematic errors. Possible other systematic effects due to a different irradiation geometry or the different deuteron energy have been reduced largely as the two data sets are in very good agreement.

Table 2. Final results for the ^{27}Al(n,2n)^{26g}Al reaction cross-sections as determined from ^{26}Al/^{27}Al ratios and neutron fluences (see eq. (2)). Averaged cross-section data are listed as a function of neutron energy.

E_n (MeV)	Cross-section (mb)	Irradiation place
13.67 ± 0.04	0.03 ± 0.04	Vienna
13.68 ± 0.05	0.15 ± 0.10	St. Petersburg
13.71 ± 0.04	0.20 ± 0.06	Vienna
13.74 ± 0.04	0.52 ± 0.10	St. Petersburg
13.74 ± 0.04	0.58 ± 0.10	St. Petersburg
13.77 ± 0.04	0.8 ± 0.1	Vienna
13.85 ± 0.04	2.5 ± 0.3	Vienna
13.87 ± 0.03	3.1 ± 0.4	St. Petersburg
13.89 ± 0.04	3.3 ± 0.4	Vienna
13.98 ± 0.03	5.4 ± 0.4	Vienna
14.07 ± 0.02	6.7 ± 0.5	St. Petersburg
14.09 ± 0.02	7.8 ± 0.5	Vienna
14.15 ± 0.02	9.8 ± 0.7	Vienna
14.28 ± 0.02	13.0 ± 0.9	Vienna
14.29 ± 0.02	12.5 ± 0.8	St. Petersburg
14.41 ± 0.02	17.3 ± 0.9	Vienna
14.48 ± 0.03	18.5 ± 1.3	St. Petersburg
14.51 ± 0.02	20.0 ± 1.3	Vienna
14.61 ± 0.02	23.5 ± 1.3	Vienna
14.70 ± 0.04	24.2 ± 1.8	St. Petersburg
14.70 ± 0.04	25.3 ± 1.3	St. Petersburg
14.73 ± 0.02	27.1 ± 1.5	Vienna
14.80 ± 0.05	29.0 ± 2.0	Tokai-mura
14.83 ± 0.02	30.8 ± 1.6	Vienna
14.84 ± 0.06	30.6 ± 1.8	St. Petersburg
17.0 ± 0.1	83 ± 6	Tübingen
17.0 ± 0.1	85 ± 6	Tübingen
19.0 ± 0.1	96 ± 7	Tübingen
19.0 ± 0.1	105 ± 7	Tübingen

Al samples irradiated in Tokai-mura were used to produce an independent Al metal standard for the AMS measurements (see sect. 2.2). In addition, the cross-section could also be deduced since the mean neutron fluence was known. Due to the close distance of the irradiated Al samples to the neutron producing Ti-T target, a considerable change of the neutron fluence in the Al foils occurred. Therefore, tiny cut-outs of the foil area were used for the AMS measurements. A total of 81 samples were measured. The individual isotope ratios were averaged and compared with the mean isotope ratio obtained from the activity measurement. The close distance of the Al foils to the Ti-T target resulted in a somewhat larger uncertainty (7%) in the cross-section data (see table 2).

The solid line in fig. 4b is a 3rd-order (least-squares) fit onto the averaged data points from samples irradiated in Vienna (below 14.6 MeV neutron energy a very similar result is obtained from a 2nd-order fit; however, for neutron energies of 14.6 MeV and higher, the excitation function tends to become more linear). The 3rd-order fit represents a very smooth trend down to the lowest cross-sections. This fit (without any constraints) approaches a cross-section value of zero for a neutron energy of 13.67 MeV.

Table 3. Summary of the various contributions (in %) to the total uncertainty of the cross-section values. Presented is the case for data obtained from samples irradiated in Vienna. For "St. Petersburg samples" similar values were obtained. The uncertainty from the AMS measurements as well as the resulting uncertainty of the cross-section data from the uncertainty of the corresponding neutron energy are shown for three cases. The last line summarizes the total uncertainty from the 17 and 19 MeV data. The last column lists the total uncertainty calculated from the square root of the sum of the squared random and systematic contributions. In table 2 all these contributions are included.

	Source of uncertainty					
	RANDOM		error (%)	SYSTEMATIC	error (%)	TOTAL (%)
Neutron fluence	Counting statistics		< 1.0	Branching ratio	< 0.5	
	Sample mass (Nb)		< 0.5	Detector efficiency	1.4	
	Position of Al samples		< 1.0	Half-life of ^{92m}Nb	< 0.5	
				Neutron scattering	< 1.0	
				σ (^{93}Nb(n,2n)^{92m}Nb)	1.3	
				Flux variation	< 0.5	
	Total		< 1.5		$\leqslant 2.3$	$\leqslant 2.7$
AMS	Counting statistics	13.8 MeV	≈ 10	^{26}Al/^{27}Al ratio of Al standard	3.5	
		14.2 MeV	≈ 4			
		14.7 MeV	≈ 1.5			
	Background correction	13.8 MeV	≈ 3			
		14.2 MeV	< 1			
		14.7 MeV	< 1			
	Normalization factor		< 0.5			
	Total		1.5–10.5		3.5	3.8–11
E_n		13.8 MeV	≈ 50			
		14.2 MeV	≈ 5			
		14.7 MeV	≈ 2.5			
Total error 14 MeV		13.8 MeV	≈ 51			51
		14.2 MeV	< 7		4.3	$\leqslant 8$
		14.7 MeV	< 3.2			$\leqslant 5.5$
Total error 17/19 MeV		17/19 MeV	3.8		5.8	7.0

This "threshold" energy lies 0.12 MeV higher than the theoretical one calculated from the mass difference using the data from [28]. Due to the uncertainty in the absolute neutron energy and the absolute uncertainty of the cross-sections (see table 2) in this region it is not possible to decide whether this deviation is significant (*e.g.*, the population of the 3^+ excited state in ^{26}Al may influence the shape of the excitation function in the immediate vicinity of the threshold).

The final cross-section data are presented in table 2. The total error listed consists of random and systematic (4.5%) contributions. The error from the uncertainty of the neutron energy (not included in column 2) becomes significant in the near-threshold region (see below).

Overall, the results from samples irradiated under different conditions in the three labs show a remarkably good agreement. In the near-threshold region the difference is less or equal 0.5 mb, and for the highest cross-sections the difference is lower than 2.5% (see fig. 4b).

3.2 Summary of the uncertainty contributions

The individual contributions to the total uncertainty are shown in table 3. The uncertainty of the neutron fluence amounts to $\leqslant 2.7$%. The uncertainty of the ^{26}Al/^{27}Al ratios comes mainly from the uncertainty of the nominal values of the ^{26}Al standard material (3.5%) and from averaging of the individual results over the whole sample area as well as statistical errors. The latter dominate the low isotope ratios, whereas systematic errors affect the higher cross-sections.

The neutron energy in the near-threshold region was assumed to be known to better than 40 keV. This leads to an additional uncertainty of 0.8 mb for a neutron energy of 13.8 MeV. It corresponds to an error of about 50% at 13.8 MeV, and about 25% at 13.9 MeV and reflects the steeply raising shape of the excitation function near threshold. For the higher-energy region, a 20 keV uncertainty was assumed, which corresponds to absolute uncertainties of 0.6 mb, *i.e.* 10% at 14.0 MeV neutron energy

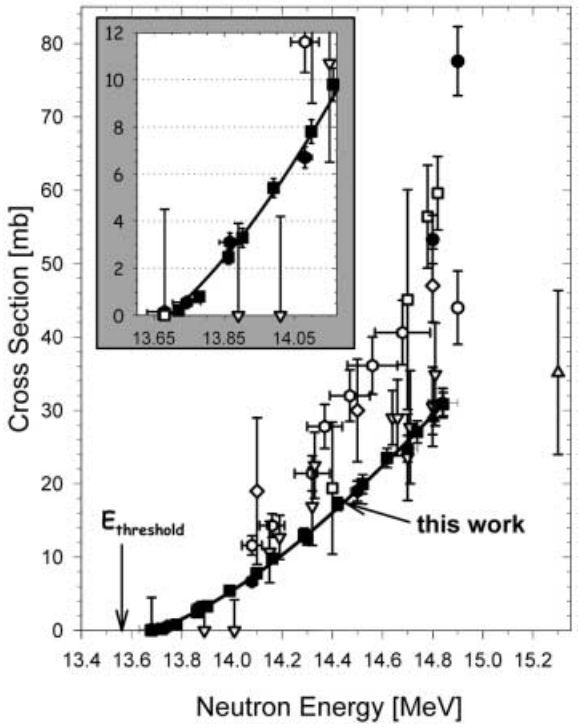

Fig. 5. Comparison of the ^{27}Al(n,2n)^{26g}Al cross-section data obtained in this work (Vienna, St. Petersburg and Tokai-mura samples) with previous experiments (see fig. 2). The insert shows more clearly the improvement in the knowledge of this excitation function near threshold.

and 2.4% for 14.8 MeV. The assumption of an uncertainty of 20 keV is supported by the fact that for the irradiation in Vienna both hemispheres (see fig. 2) were used agreeing very well with each other. The energy check with the Zr-Nb method as well as the data from the irradiation in St. Petersburg, supports this, too.

3.3 Comparison of the new ^{27}Al(n, 2n)^{26g}Al cross-sections with previous results

The new data show a substantial improvement over previous measurements (see fig. 5). Since the results from the three neutron irradiations (Vienna, St. Petersburg and Tokai-mura) for 14 MeV neutrons agree very well with each other, one can safely assume that systematic errors in the neutron irradiation have been largely eliminated. The absolute values of the cross-sections are believed to be known to about 5–8% in the energy region above 14 MeV. The uncertainty stems mainly from systematic errors. Overall, a very consistent set of cross-section data was obtained from the samples irradiated under these different conditions.

No clear trend for the shape of the excitation function could be deduced from previous results. Both a pure quadratic and a pure linear shape of the excitation function were in principle possible from these data. The new data indeed indicate a combination of this parameterization. For higher neutron energies the excitation function tends to become more linear and a third power dependence becomes important.

Below 14 MeV neutron energy only upper limits (lower than 4 mb) were given in the previous publications (cf. fig. 2). A good agreement with the data of Sasao *et al.* [9] was obtained. However, their uncertainties are a factor of 5 larger. The cross-section data of Ikeda *et al.* [11] and Smither and Greenwood [1,7,8] are generally higher, about a factor of 2 for the higher neutron energies. Below a neutron energy of 14.4 MeV their data are consistent with those of this work, but only due to their large errors. The data of Iwasaki *et al.* [10] are also about a factor of two higher. Their uncertainty was assumed to be smaller than that of the two above-mentioned results. Both results (Iwasaki *et al.* and Sasao *et al.*) were obtained from activity measurements. The data of Zhao *et al.* [13] for neutron energies of 14.8 and 14.9 MeV, are clearly inconsistent with the results of this work. Also data of Nakamura *et al.* [12] are shown. The cross-section data obtained in this work support this lower trend of the ^{27}Al(n,2n)^{26}Al excitation function as indicated by [12].

3.4 Cross-sections for 17 and 19 MeV neutron energies

For both neutron energies (17 and 19 MeV) two Al foils were available. About 10 samples per foil were prepared for AMS measurements. The main contributions to the uncertainty of the cross-section values are 4.7% from the fluence determination and 5% from the AMS measurements (isotope ratios in the order of 10^{-13}). The total error of the cross-section data amounts to 7%. The uncertainty of the neutron energy is negligible due to the nearly energy-independent shape of the excitation function in this energy region.

In fig. 6 a comparison with available evaluations [14] is shown (see also fig. 2). The most recent one, ENDF/B-VI, is in good agreement with our data. JEF-2 shows about the same trend as ENDF/B-VI for energies lower than 16 MeV. The other evaluations (JENDL and FENDL-A) disagree with our results, and in particular the precursor of the recent ENDF-file, namely ENDF/B-V. They reflect some of the previously measured data. It is obvious that our improved data set allows a clear selection among these different attempts to describe the excitation function with semi-empirical methods.

4 Sensitivity of the ^{27}Al(n,2n)^{26g}Al reaction for monitoring the ion temperature in a D-T fusion plasma

4.1 Maxwellian D-T fusion plasma

With the improved knowledge of the excitation function obtained in this work, its sensitivity for monitoring the ion temperature in a D-T fusion plasma was investigated.

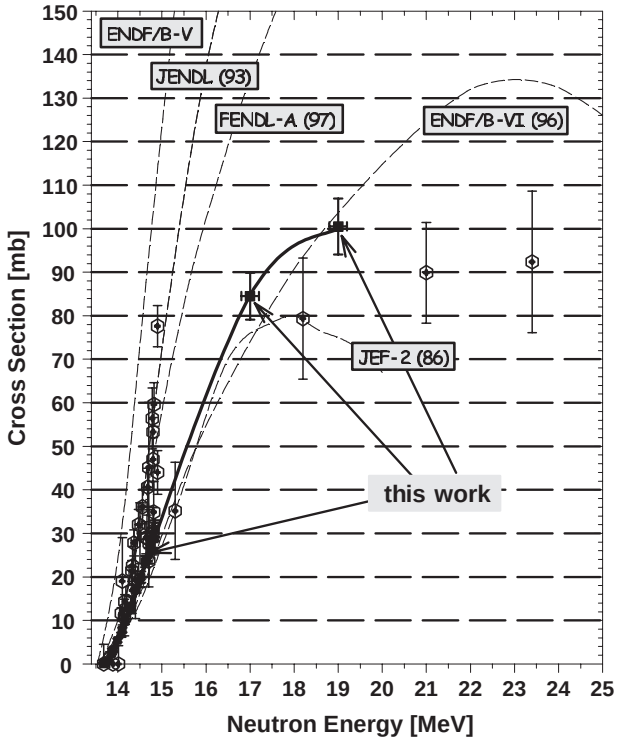

Fig. 6. Comparison of the ^{27}Al(n,2n)^{26g}Al cross-section data obtained in this work with previous experiments and evaluations for the whole energy region investigated. The dashed line is a 3rd-order fit (least-squares) to the new data. The best agreement was found with the recent ENDF/B-VI evaluation. The experimental data of Sasao *et al.* [9] in the near-threshold region and data of Nakamura *et al.* [12] agree with the data obtained in this work (cf. fig. 5) The experimental data above 15 MeV neutron energy (diamonds) are from [12].

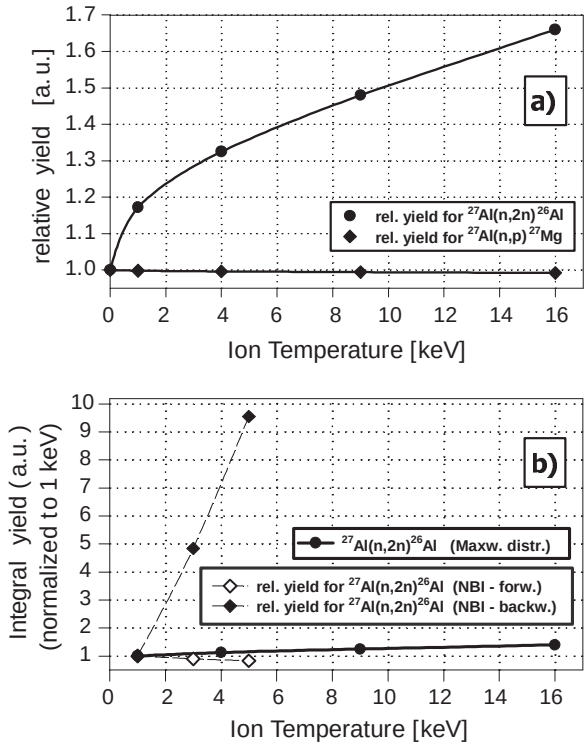

Fig. 7. In part a) the sensitivity of the ^{27}Al(n,2n)^{26g}Al and the ^{27}Al(n,p)^{27}Mg reaction to changes of the ion temperature is plotted. A Maxwellian distribution for the velocity distribution of the reactants in the plasma was assumed. The total yield of product nuclei ^{26}Al and ^{27}Mg was normalized to the value obtained for an ion temperature approaching 0 keV and to the same total neutron yield ("per source neutron"). In part b) also the sensitivity of the ^{27}Al(n,2n)^{26g}Al reaction for neutral beam injection (NBI) is shown for two viewing directions (diamonds). For both, forward (forw.) and backward (backw.) viewing the change of the total yield is plotted.

Different ion temperatures result in different neutron spectral distributions [29]. As the fusion product energy spectra are almost perfectly Gaussian, they can be characterized by a systematic energy shift (D) and their FWHM. The most pronounced feature of these spectra is that the FWHM $w_{1/2}$, to first order, is proportional to the square root of the plasma temperature ($w_{1/2} = 177.2\sqrt{T_i}$ for the D-T reaction, where T_i and $w_{1/2}$ are in units of keV [30]). The width is therefore a direct measure of the ion temperature. In the case of the T(d,n)^{4}He reaction, for an ion temperature of 16 keV, the centroid of the neutron energy lies only 46 keV or 3% above that for temperatures of 1 keV (14.06 MeV) but the width has increased by a factor of 4 (see fig. 1).

In thermal equilibrium, a Maxwellian distribution for the velocity distribution of the reactants in the plasma was assumed. The neutron spectral distributions were calculated from a parameterization of ref. [31] or directly taken from ref. [1]. If the Maxwellian is distorted at the high-energy tail (*e.g.*, interaction with material), the production rate and the distribution may change significantly. Not considered is this alteration of the original neutron spectra via interaction of neutrons with first wall and blanket material in a fusion device (see [32,33])

The change in the total yield of produced ^{26}Al nuclei *per source neutron* with increasing ion temperature is a measure of the sensitivity of this method. This sensitivity of the ^{27}Al(n,2n)^{26}Al reaction to changes in the plasma temperature is shown in fig. 7a. If the ion temperature is changed from 1 keV to 16 keV, the yield of ^{26}Al nuclei increases by about 45% per source neutron. The total neutron yield, of course, increases by 5 orders of magnitude due to its proportionality to the reactivity. This change in the total neutron yield may easily be determined from a temperature-insensitive reaction (*e.g.*, a linear reaction) whose production rate is directly proportional to the neutron fluence, like the ^{27}Al(n,p)^{27}Mg reaction (case 1 in fig. 1).

4.2 Uncertainty of this method

For an absolute determination of the plasma temperature absolute cross-sections are necessary. For monitoring changes of the ion temperature only the slope of the excitation function is of importance. The influence of the

uncertainty of the ^{27}Al(n,2n)^{26}Al excitation function was estimated by varying the slope of the fit to the data within the experimental uncertainty (5%). The whole excitation function was also shifted slightly to higher and lower energies taking into account the uncertainty of the neutron energy.

For an absolute determination of the ion temperature, uncertainties of 5% for the absolute value of the cross-section data, and 2% for the yield determination (*e.g.*, from AMS measurement) were assumed. For monitoring the ion temperature the slope of the excitation function is reproduced to better than 1% from our measurements; therefore the uncertainty is mainly given by the 2% for the yield determination. For typical ion temperatures of 10–20 keV this method allows temperature monitoring to an accuracy of better than 10%. For high neutron fluxes, ^{26}Al/^{27}Al isotope ratios in the order of 10^{-10} and higher can be obtained easily. Utilizing AMS for the determination of the number of produced ^{26}Al nuclei, statistical errors will be negligible. For monitoring the temperature, improving the accuracy of the yield determination to about 1% also lowers the uncertainty of the temperature by a factor of 2.

A threshold energy close to the centroid of the neutron spectral distribution is required for a nuclear reaction, in order to be sensitive to changes in the temperature of a fusion plasma. Possible other candidates were investigated, too. One candidate is the ^{54}Fe(n,2n)^{53}Fe reaction [1,8] with a theoretical threshold energy of 13.63 MeV. But the uncertainties, due to the scattering of the individual experiments represent a similar status as the one for the Al excitation function before this work. However, both, production cross-sections and decay properties of ^{53}Fe are less favorable.

4.3 Non-Maxwellian D-T fusion plasma

Many of the present fusion experiments are characterized by substantial "auxiliary" heating (*e.g.*, neutral beam injection or radio-frequency heating). In case of non-equilibrium plasmas with non-Maxwellian velocity distributions of the ions, a non-Gaussian form of the neutron spectral distribution results. For anisotropic plasmas, depending on the direction of viewing, *e.g.*, relative to the direction of the injected beam, the spectral distribution is shifted and distorted. In direction of the incoming beam the centroid of the distribution is shifted to higher energies. Looking parallel, the centroid is shifted to lower energies.

Smither *et al.* [8] have discussed the measurement of ion temperatures in the case of neutral beam injection using the ^{27}Al(n,2n)^{26g}Al and the ^{54}Fe(n,2n)^{53}Fe reactions. Their neutron spectral distributions calculated for three ion temperatures (1, 3 and 5 keV with neutral beam injection of deuterium with an energy of 120 keV) were used for the following estimations, too. These energy distributions were also mirrored at a neutron energy of 14.1 MeV (mean neutron energy from a thermal plasma approaching a temperature of 0 keV) to simulate colinear viewing. For both cases (forward and backward viewing) the product of the ^{27}Al(n,2n)^{26g}Al reaction cross-sections with the corresponding neutron spectral distributions, were calculated.

In fig. 7b the resulting sensitivity is shown for forward and backward viewing. Here, the above-mentioned characteristics, namely the increase in sensitivity with threshold energy approaching the centroid of the neutron energy distribution is clearly shown. The integral yield was normalized in each case to the value obtained for an ion temperature of 1 keV. For anti-parallel viewing, not much changes. For parallel viewing a substantial increase in the total yield is observed for higher temperatures. The centroid of the spectral distribution was assumed to be at about 13.5 MeV. The threshold of the ^{27}Al(n,2n)^{26g}Al reaction lies at 13.55 MeV. Only that part of the neutron spectral distribution, that lies above this threshold energy, contributes to the total yield. This amount of neutrons increases strongly with higher ion temperatures. In combination with the very strongly varying ^{27}Al(n,2n)^{26}Al excitation function near threshold, the total amount of produced ^{26}Al nuclei increases by about a factor of 10 for a change in the plasma temperature from 1 to 5 keV. An uncertainty of 5% in the determination of the total yield leads to an uncertainty in the ion temperature of 0.2 keV only.

Once, a calibration of the required accuracy is established, this reaction represents a very sensitive measure of changes in the neutron spectral distribution. The total production yield is lower in this case but the high neutron fluences in fusion devices in combination with the very sensitive method of AMS, makes this reaction useful as a diagnostic tool in fusion technology.

5 Summary

A detailed measurement of the ^{27}Al(n,2n)^{26g}Al reaction cross-sections was performed in the near-threshold region ($E_{\mathrm{th}} = 13.54$ MeV), and its possible applicability for ion temperature measurements was investigated. It has been pointed out by Smither and Greenwood [1] that this reaction can be used as a monitor to determine the ion temperature in a D-T fusion plasma. Al samples were irradiated with 14 MeV neutrons generated via the T(d,n)^{4}He reaction at three different laboratories under different conditions. The produced ^{26}Al was measured using the extremely sensitive method of accelerator mass spectrometry (AMS). ^{26}Al/^{27}Al isotope ratios as low as 10^{-15} could be measured with the Vienna Environmental Research Accelerator (VERA) corresponding to cross-section values as low as 0.04 mb.

The results from the different neutron irradiations agree very well with each other. The absolute cross-section values could be measured to 5% (mainly systematic errors). The slope of the excitation function is reproduced to better than 1% from our measurements. For monitoring the ion temperature of a thermal plasma a sensitivity of a few percent can be achieved by this method. In case of non-thermal plasmas depending on the observation angle a very sensitive measure of changes can be achieved.

In addition, well above threshold, Al samples have been irradiated at 17 and 19 MeV neutron energy. Analogous to the measurements near threshold, the amount of long-lived ^{26}Al nuclei produced during this irradiation has been measured via AMS. This data confirm again a lower trend of the excitation function and they are in good agreement with ENDF/B-VI.

We believe that our measurements provide the basic ingredients for a "plasma thermometer" using the ^{27}Al(n,2n)^{26g}Al reaction. Therefore, it would be very interesting to apply this method for a D-T fusion plasma temperature measurement.

We would like to thank P. Kubik, E. Nolte, and S. Vogt for supplying valuable standard materials for the AMS measurements.

References

1. R.K. Smither, L.R. Greenwood, J. Nucl. Mater. **122** & **123**, 1071 (1984).
2. S. Fetter, E.T. Cheng, F.M. Mann, Fus. Eng. and Des. **13**, 239 (1990).
3. C. Gomes, D.L. Smith, E.T. Cheng, *Proceedings of the 13th Topical Meeting on the Technology of Fusion Energy*, Fusion Technol. **34**, No. 3-2, 706 (1998).
4. A. Wallner, S.V. Chuvaev, A.A. Filatenkov, W. Kutschera, G. Mertens, A. Priller, W. Rochow, P. Steier, H. Vonach, *Proceedings of the International Conference on Nuclear Data for Science and Technology, Trieste, 19-24 May 1997*, edited by G. Reffo, A. Ventura, C. Grandi, SIF Conf. Proc. **59**, (Editrice Compositori, Bologna, 1998) p. 1248.
5. A. Wallner, PhD Thesis, University of Vienna (2000).
6. N.E. Holden, Pure Appl. Chem. **62**, 941 (1990).
7. R.K. Smither, L.R. Greenwood, Report ANL-CMTI-8556(1983), p. 20-28.
8. R.K. Smither, L.R. Greenwood, H. Hendel, Rev. Sci. Instrum. **56**, 1078 (1985).
9. M. Sasao, T. Hayashi, K. Taniguchi, A. Takahashi, T. Iida, Phys. Rev. C **35**, 2327 (1987).
10. S. Iwasaki, J.R. Dumais, K. Sugiyama, *Proceedings of the International Conference on Nuclear Data for Science and Technology, Mito, May 30-June 3, 1988*, edited by S. Igarashi (Saikon Publishing Co., Tokyo, 1988) p. 295; S. Iwasaki, N. Odano, J.R. Dumais, *Proceedings of the 15th International Symposium on Fusion Technology, Utrecht, Sept. 19-23, 1988* (Elsevier Science Publishers B.V., North Holland, Amsterdam, 1989).
11. Y. Ikeda, D.L. Smith, A. Kumar, C. Konno, Report JAERI-M-91-032 (1991), p. 272; Y. Ikeda, A. Kumar, C. Konno, *Proceedings of the International Conference on Nuclear Data for Science and Technology, Jülich, 13-17 May 1991* (Springer Verlag, Berlin, Heidelberg, New York, 1992) p. 364.
12. T. Nakamura, H. Sugita, M. Imamura, Y. Uwamino, H. Nagai, K. Kobayashi, Phys. Rev. C **43**, 1831 (1991); T. Nakamura, H. Sugita, M. Imamura, Y. Uwamino, S. Shibata, H. Nagai, M. Takabatake, K. Kobayashi, *Proceedings of the International Conference on Nuclear Data for Science and Technology, Jülich, 13-17 May 1991* (Springer Verlag, Berlin, Heidelberg, New York, 1992) p. 714.
13. Q. Zhao, X. Lu, Z. Guo, Z. Shi, J. Wang, K. Liu, B. Li, K. Li, J. Chen, H. Lu, Chin. Phys. Lett. **15**, 8 (1998).
14. ENDF/B-VI-evaluation (1996), FENDL (1997), JEF-2 (1986), and JENDL-3.2 (revised 1993), see IAEA-ENDF entry 1325-1451 and webpage: `http://www-nds.iaea.org`.
15. M. Wagner, H. Vonach, A. Pavlik, B. Strohmaier, S. Tagesen, J. Martinez-Rico, Report Physik Daten - Physics Data **13-5**, Fachinformationszentrum Karlsruhe (1990).
16. A. Pavlik, G. Winkler, Report INDC(AUS)-011/LI, IAEA Nuclear Data Section, Vienna (1986).
17. V.E. Lewis, K.J. Zieba, Nucl. Instrum. Methods **174**, 141 (1980).
18. A.A. Filatenkov, S.V. Chuvaev, V.N. Aksenov, V.A. Jakovlev, Report INDC(CCP)-402, IAEA, Vienna (1997).
19. A.A. Filatenkov, S.V. Chuvaev, V.A. Jakovlev, V.P. Popik, Fus. Eng. and Des. **37**, 151 (1997).
20. C. Konno, Y. Ikeda, K. Oishi, K. Kawade, H. Yamamoto, H. Maekawa, Report JAERI 1329, Japan Atomic Energy Research Institute (1993).
21. A. Wallner, Y. Ikeda, W. Kutschera, A. Priller, P. Steier, H. Vonach, E. Wild, Nucl. Instrum. Methods B **172**, 382 (2000).
22. S. Tagesen, H. Vonach, A. Wallner, IAEA-report, International Atomic Energy Agency, Nuclear Data Section, INDC(AUS)-016, 2002.
23. W. Kutschera, P. Collon, H. Friedmann, R. Golser, P. Hille, A. Priller, W. Rom, P. Steier, S. Tagesen, A. Wallner, E. Wild, G. Winkler, Nucl. Instrum. Methods B **123**, 47 (1997).
24. A. Priller, R. Golser, P. Hille, W. Kutschera, W. Rom, P. Steier, A. Wallner, E. Wild, Nucl. Instrum. Methods B **123**, 193 (1997).
25. A. Wallner, R. Golser, W. Kutschera, A. Priller, P. Steier, H. Vonach, E. Wild, Nucl. Instrum. Methods B **139**, 301 (1998).
26. J.A. Ferry, Nucl. Instrum. Methods A **328**, 28 (1993).
27. S. Vogt, M.-S. Wang, R. Li, M. Lipschutz, Nucl. Instrum. Methods B **92**, 153 (1994).
28. G. Audi, A.H. Wapstra, Nucl. Phys. A **595**, 409 (1995).
29. H. Brysk, Plasma Phys. **15**, 611 (1973).
30. O.N. Jarvis, Plasma Phys. Control. Fusion **36**, 209 (1994).
31. L. Ballabio, G. Gorini, J. Källne, Rev. Sci. Instrum. **68**, 585 (1997); L. Ballabio, J. Källne, G. Gorini, Nucl. Fusion **38**, 1723 (1998).
32. C.W. Barnes, A.R. Larson, A.L. Roquemore, Fusion Technol. **30**, 63 (1996).
33. L.C. Johnson, C.W. Barnes, A. Krasilnikov, F.B. Marcus, T. Nishitani, and the ITER Joint Central Team and Home Teams, Rev. Sci. Instrum. **68**, 569 (1997).